Materials Chemistry and Physics 121 (2010) 302–307

Contents lists available at ScienceDirect

Materials Chemistry and Physics

journal homepage: www.elsevier.com/locate/matchemphys

The preparation and electrochemical performances of $LiFePO_4$-multiwalled nanotubes composite cathode materials for lithium ion batteries

Yan Feng*

College of Chemistry and Life Science, Tianjin Key Laboratory of Structure and Performance for Functional Molecule, Tianjin Normal University, No. 393 Binshuixidao Street, Xiqing District, Tianjin 300387, PR China

ARTICLE INFO

Article history:
Received 13 February 2009
Received in revised form 2 November 2009
Accepted 21 January 2010

Keywords:
Composite materials
Annealing
X-ray diffraction topography
Electrochemical properties

ABSTRACT

$LiFePO_4$-MWCNTs (multi-walled carbon nanotubes) composite cathode materials were prepared by mixing $LiFePO_4$ and MWCNTs in ethanol followed by heat-treatment at 500 °C for 5 h. The structural, morphology and electrochemical performances of $LiFePO_4$-MWCNTs composite materials were investigated by X-ray diffraction (XRD), scanning electron microscopy (SEM), transmission electron microscopy (TEM), galvanostatic charge–discharge cycle tests, cyclic voltammetry (CV) and electrochemical impedance spectroscopy (EIS). The results indicated that MWCNTs adding improved the electronic conductivity, the discharge capacity, cycle stability and lithium ion diffusion kinetics of $LiFePO_4$, but MWCNTs adding did not charge the orthorhombic olivine-type structure of $LiFePO_4$. In all these prepared $LiFePO_4$ with x wt.% MWCNTs ($x = 4, 7, 10$) composites, 7 wt.% MWCNTs adding composite cathode shows the best electrochemical performance, which gets an initial discharge capacity of 152.7 mAh g^{-1} at 0.18 C discharge rates with capacity retention ratio of 97.77% after 100 cycles.

© 2010 Elsevier B.V. All rights reserved.

1. Introduction

Rechargeable lithium ion batteries exhibiting high energy and high power density are in great demand as energy sources for a variety of advanced devices such as cellular phones, notebook computers and electric/hybrid vehicles [1]. However, the development and application of lithium ion batteries are mainly limited by the cathodes [2]. At present, the most widely used commercial cathode material for lithium ion battery is $LiCoO_2$ due to its ease of production, stable electrochemical cycling and acceptable specific capacity [3–5]. This cathode was successful, but serious problems such as safety, cost and toxicity still remained unsolved. Possible alternatives are $LiMn_2O_4$ [6–13], $Li[Ni_{1/3}Mn_{1/3}Co_{1/3}]O_2$ [14–20], LiV_3O_8 [21,22] and $LiFePO_4$ [23–40] etc.

Among these cathode materials, olivine structured $LiFePO_4$ have attracted the most interest due to the low cost, low toxicity and the high approaching to the theoretical, practical capacity of larger than 160 mAh g^{-1} at low rates with flat charge–discharge potential plateaus around 3.4 V vs. Li^+/Li owing to the Fe^{3+}/Fe^{2+} redox couple [27]. However, the low electronic conductivity (10^{-8} to 10^{-10} S cm^{-1}) of $LiFePO_4$ made it difficult to utilize the full theoretical capacity at useful rate. To overcome this problem, tremendous efforts have been made, such as doping with foreign atom [25,26,29–31], decreasing the particle size [24,27] and coating electronically conductive reagent [23,28], etc.

Carbon nanotubes are readily electronic conductive [33,34]. Li et al. [32], Liu et al. [35] and Sheem et al. [36] applied MWCNTs as the conducting additive in $LiFePO_4$ and $LiCoO_2$ electrodes. They demonstrated MWCNTs were better conductor than carbon black. The reversible discharge capacity of $LiFePO_4$-MWCNTs composite cathode was 150 mAh g^{-1} at 0.1 C rates while the $LiFePO_4$-carbon black composite was 140 mAh g^{-1} at the same rate [32]. Compared with the batteries carbon black additive, those with CNT additive show better electrochemical performances with capacity retention ratio of 99.2% after 50 cycles at 0.1 C rates. Chen and Whittingham [37] and Gu and co-workers [38] prepared $LiFePO_4$-MWCNTs via hydrothermal method and indicated that the added MWCNTs in pure $LiFePO_4$ enhanced the electronic conductivity of the final product. Wang et al. [39] prepared $LiFePO_4$-MWCNTs by microwave routes and indicated and the electrochemical capacity of $LiFePO_4$-MWCNTs was 145 mAh g^{-1} at 0.5 C rates and cycle ability was stable. However, these above methods were not convenient and most of these need more than two heating process.

In this work, a liquid mixing method followed by heat-treating was used to prepare $LiFePO_4$-MWCNTs composite cathodes. The mixing process of $LiFePO_4$ and MWCNTs was simple and the following heating process was easy to control. The structural, morphological and electrochemical properties of the $LiFePO_4$-MWCNTs composite were investigated.

* Tel.: +86 22 23766515; fax: +86 22 23766515.
E-mail address: fengyan@tju.edu.cn.

0254-0584/$ – see front matter © 2010 Elsevier B.V. All rights reserved.
doi:10.1016/j.matchemphys.2010.01.038

Samsung Ex. 1042, Page 1 of 6
Samsung Electronics Co., Ltd., et al. v. Molecular Rebar Design, LLC
IPR2025-00356

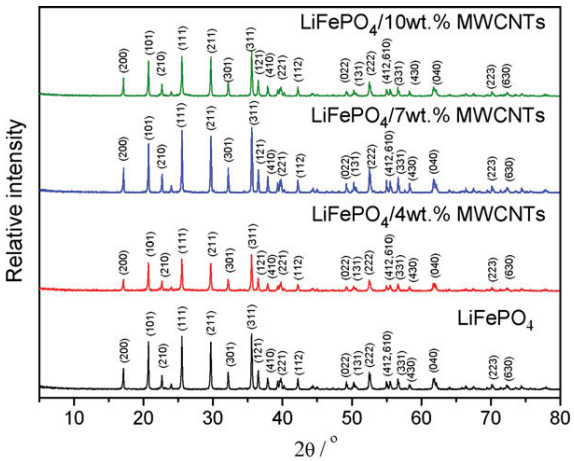

Fig. 1. XRD patterns of $LiFePO_4$ and $LiFePO_4$-MWCNTs.

2. Experimental

$LiFePO_4$ was prepared from stoichiometric amount of $LiOH{\cdot}H_2O$, $FeC_2O_4{\cdot}2H_2O$ and $NH_3H_2PO_4$ (molar ratio 1:1:1, respectively). The mixture was ball milled for 1 h and pre-pyrolyzed at 400 °C for 5 h in pure argon flow. The resulting product was reground by ball milling for 1 h and then heated at 700 °C for 16 h in pure argon flow. MWCNTs (Shenzhen Nanotech Port, China) were soaked in concentrated nitric acid and refluxed for 5 h. The product was washed by distilled water and acetone, and then dried in a vacuum at 60 °C. As-treated MWCNTs and as-prepared $LiFePO_4$ were mixed in absolute alcohol at 60 °C with vigorous stir (the weight content of MWCNTs adding was 4, 7, 10 wt.% of $LiFePO_4$). Until all the liquid was evaporated, the solid was dried in a vacuum at 120 °C for 1 h and then heated at 500 °C for 5 h in pure argon flow. The resulting composite powder was ground in agate mortar to obtain objective product.

The phase structures of the $LiFePO_4$-MWCNTs composite and pure $LiFePO_4$ were analyzed by X-ray diffraction (XRD) using Rigaku X-ray powder diffractometer D/MAX-2500 with graphite monochromatic CuKα radiation in the 2θ range of 3–80°. Morphologies of the composite were investigated by Shimadzu SS-550 scanning electron microscopy (SEM) with an accelerating voltage of 15 kV. Transmission electron microscopy (TEM) images were collected by using PHILIPS Tecnai G^2 F20 (operating at 200 kV) transmission electron microscopes. The electronic conductivities of all prepared samples are measured with the four-electrode method by SDY-5 four-point probe meter (Guangzhou, China).

For electrochemical tests, cathode electrodes were prepared by mixing the active material ($LiFePO_4$-MWCNTs), conductive additive (acetylene black, ENSACO, Switzerland) and binder (PTFE, Sigma Aldrich, China) in a weigh ratio of 85:10:5, respectively. The materials, as a cathode, were assembled into lithium batteries in an argon filled glove box, with the use of Celgard 2300 as a separator, Li foil as counter and reference electrodes, and 1 mol dm^{-3} $LiPF_6$ in ethylene carbonate (EC), propylene carbonate (PC) and dimethyl carbonate (DMC) (1:1:1 by volume respectively, Jinniu, China) as electrolyte, to form laboratory-made coin-type cells (size: CR 2032). Galvanostatic charge–discharge cycle tests were performed on a LAND 2001A battery testing system (Jinnuo, China) in the potential range of 2.5–4.3 V respectively vs. Li^+/Li. Cyclic voltammetry (CV) tests were performed on a CHI 660C electrochemical workstation (Chenhua, China) at a scan rate of 0.1 mV S^{-1} at a potential interval 2.5–4.3 V vs. Li/Li^+. Electrochemical impedance spectroscopy (EIS) was also performed on a CHI 660C electrochemical workstation. The EIS measurement conditions were: AC amplitude 5 mV; testing potential 3.4 V vs. Li^+/Li at approximate 50% DOD (depth of discharge); frequency range 10^5–0.1 Hz.

3. Results and discussion

The XRD patterns of as-prepared $LiFePO_4$ and $LiFePO_4$-MWCNTs are shown in Fig. 1. The patterns of $LiFePO_4$-MWCNTs composites can be indexed to a single-phase material having an orthorhombic olivine-type structure with a space group of *Pnma* [40], which are the same as the $LiFePO_4$ one. No diffraction peak for MWCNTs or carbon was present in either of these XRD patterns. That is because of the low content and the amorphous state of carbon in the composite materials. The XRD peak of amorphous carbon was covered by the main phases of $LiFePO_4$. Therefore, the MWCNTs adding do not change the crystal structure of pure $LiFePO_4$.

Table 1
The electronic conductivity of $LiFePO_4$ and $LiFePO_4$-MWCNTs composites.

Samples	Electronic conductivity (S cm^{-1})	
	Original materials	As-prepared electrodes
$LiFePO_4$	3.1×10^{-9}	7.4×10^{-4}
$LiFePO_4$/4 wt.% MWCNTs	5.5×10^{-4}	1.1×10^{-3}
$LiFePO_4$/7 wt.% MWCNTs	4.7×10^{-3}	5.2×10^{-3}
$LiFePO_4$/10 wt.% MWCNTs	2.3×10^{-3}	3.2×10^{-3}

Fig. 2 shows the SEM images of $LiFePO_4$ and $LiFePO_4$-MWCNTs composites. The particle size of pure $LiFePO_4$ was 1–5 μm, while that of $LiFePO_4$ with 7 wt.% MWCNTs composite was 3–5 μm. In Fig. 2d, f and h, it is clear that networks of MWCNTs appeared in the interstitial grain-boundary region, which can improve the electrical continuity between $LiFePO_4$ particles and makes the crystal structure stable. Moreover, the dispersed MWCNTs provide pathways for electron transference.

The electronic conductivity of $LiFePO_4$ with 7 wt.% MWCNTs and $LiFePO_4$ with 10 wt.% MWCNTs composite is about a factor of $\sim 10^6$ higher than the pure $LiFePO_4$, reaching to about 10^{-3} S cm^{-1} (measured by a four-point probe method, Table 1). The conductivity value of original materials and as-prepared electrode materials (active material + conductive + binder) are all shown in Table 1. The reason of the improvement of the electronic conductivity of the composite is that the MWCNTs offer the electronic transport channels in the composites. Therefore, MWCNTs adding improves the electronic conductivity of $LiFePO_4$.

Fig. 3 shows the TEM images of $LiFePO_4$, $LiFePO_4$ with 7 wt. % MWCNTs and $LiFePO_4$ with 10 wt.% MWCNTs composites. From Fig. 3a, the pure $LiFePO_4$ sample exhibits the irregular particles. From Fig. 3c, the MWCNTs coated on the surface of $LiFePO_4$ and connected the particles of $LiFePO_4$ which can be clearly seen. These results agree with SEM images in Fig. 2. The MWCNTs in the $LiFePO_4$/7 wt.% MWCNTs composite were covered around every particle of $LiFePO_4$ and they have good connection with the $LiFePO_4$ particles. The MWCNTs distribution of $LiFePO_4$/10 wt.% MWCNTs was disorderly and their orientation was lacking direction.

Discharge capacities of $LiFePO_4$ and $LiFePO_4$-MWCNTs composite at 0.18 C (1 C = 170 mA g^{-1}) are shown in Fig. 4. With the MWCNTs weight ratio increasing in the as-prepared composite, discharge capacity and cycle stability of the $LiFePO_4$-MWCNTs composite are both improved. The $LiFePO_4$ with 7 wt.% MWCNTs shows the best cycling performance among the as-prepared composites. At first cycle, the discharge capacity of $LiFePO_4$ with 7 wt.% MWCNTs is 152.7 mAh g^{-1} at 0.18 C discharge rates while that of pure $LiFePO_4$ was 141.4 mAh g^{-1}. After 100 cycles of charge–discharge, the discharge capacity of $LiFePO_4$ with 7 wt.0% MWCNTs is 149.3 mAh g^{-1} and the capacity retention is 97.77%, which are both higher than those of pure $LiFePO_4$ (125.3 mAh g^{-1} and 88.57%). That is because the MWCNTs webs covered the $LiFePO_4$ particles to protect the cathode crystal structure from distortion during charge–discharge test and also delivered good conductivity of cathode material [32,34,35].

In the case of $LiFePO_4$-MWCNTs composite, the $LiFePO_4$ with 7 wt.% MWCNTs has the best discharge capacity and cycle stability, not the 10 wt.% MWCNTs one. Here we analysis some reasons about this behavior. Firstly, Less MWCNTs content (4 wt.%) could not provide sufficient aforementioned effects and because of the little electrochemical activity of MWCNTs compared with $LiFePO_4$ active material, more MWCNTs content (such as 10 wt.%) would decrease the active material percentage leading to the decrease of discharge capacity. So the 7 wt.% MWCNTs is the best one. Additionally, from TEM images in Fig. 3d, the MWCNTs distribution of $LiFePO_4$ with 10 wt.% MWCNTs was disorderly and their orientation was lacking direction. However, the MWCNTs in the $LiFePO_4$ with

Samsung Ex. 1042, Page 2 of 6
Samsung Electronics Co., Ltd., et al. v. Molecular Rebar Design, LLC
IPR2025-00356

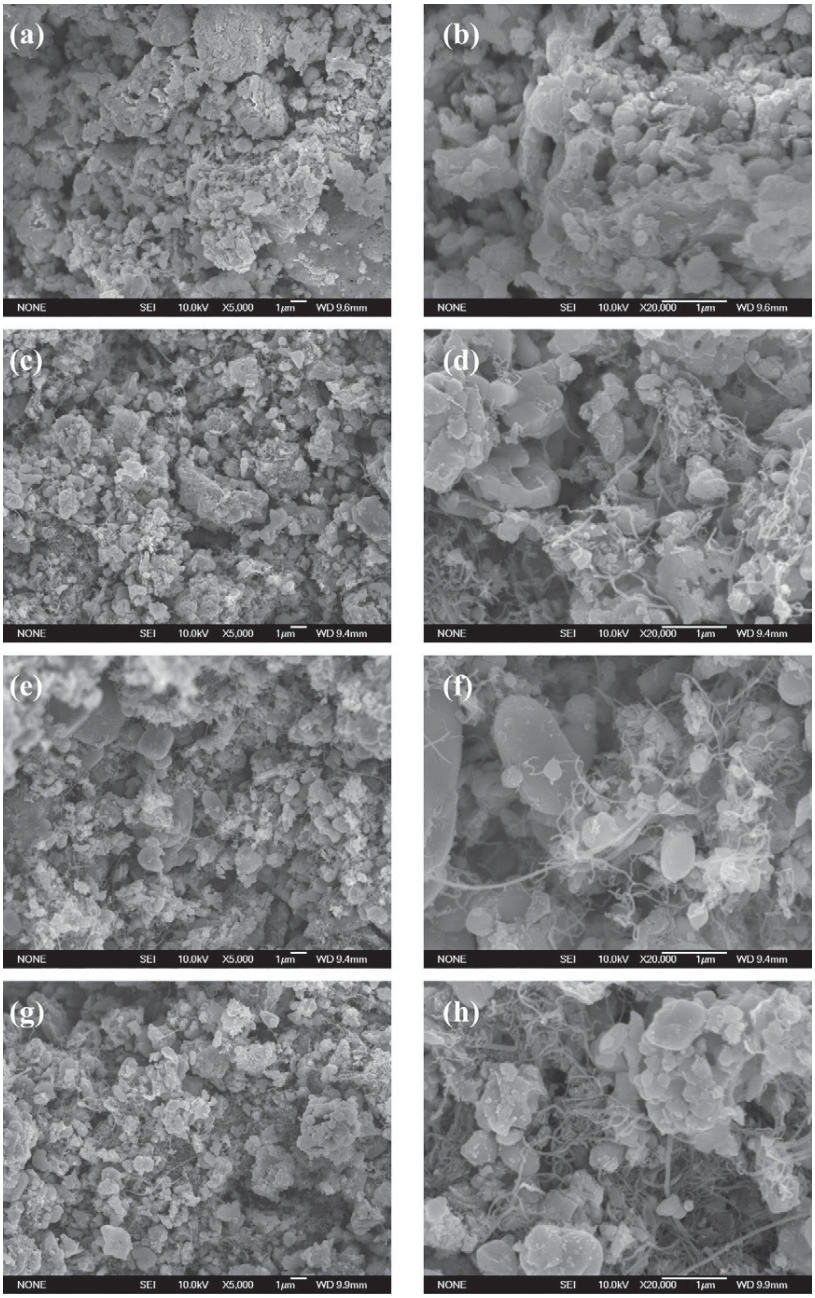

Fig. 2. SEM images of as-prepared $LiFePO_4$ (a and b), $LiFePO_4$/4 wt.% MWCNTs (c and d), $LiFePO_4$/7 wt.% MWCNTs (e and f) and $LiFePO_4$/10 wt.% MWCNTs (g and h) composites.

7 wt.% MWCNTs composite were covered around every particle of $LiFePO_4$ and they have good connection with the $LiFePO_4$ particles. The conductivity and electrochemical activity can be effectively exerted by 7 wt.% MWCNTs composite. Therefore, to get the good electrochemical performance, the 7 wt.% MWCNTs adding is the most suitable for $LiFePO_4$-MWCNTs composite.

To prove the MWCNTs adding is the main reason to protect $LiFePO_4$ structure of the electrode material during the cycling. The SEM images of 100 cycles old electrodes of $LiFePO_4$ and $LiFePO_4$-MWCNTs were investigated. From the Fig. 5a, the $LiFePO_4$ was pulverized to some extent after 100 cycles. In Fig. 5b, the particles of $LiFePO_4$ were assembled together and the particles were adhibited by each other. The pulverization lead to the structure of electrode material destroyed which cause the decreasing of the discharge capacity during the cycling. However, the $LiFePO_4$-MWCNTs composite has no such behavior. From Fig. 5c, the fringes of $LiFePO_4$-MWCNTs particles were clear and distinct, not assembled together, indicating the $LiFePO_4$-MWCNTs composite was not pulverization during the cycling. From Fig. 5d, the MWCNTs can be seen. These MWCNTs connect the big $LiFePO_4$ particles to protect the structure distortion during the cycling. Therefore, the $LiFePO_4$-MWCNTs composite has the better cycle stability than bare $LiFePO_4$ materials.

Fig. 6 shows the initial voltage profiles of the pure and the MWCNTs coating $LiFePO_4$ (0.18 C). The four samples have the similar charge–discharge curves with flat plateaus reactions but they vary in plateau voltages. The charge voltage plateau of the composite is higher than that of pure $LiFePO_4$, while the discharge voltage plateau lowers than that of pure $LiFePO_4$. For example, the charge voltage plateau is 3.47–3.57 V for $LiFePO_4$ and 3.46–4.50 V

Samsung Ex. 1042, Page 3 of 6
Samsung Electronics Co., Ltd., et al. v. Molecular Rebar Design, LLC
IPR2025-00356

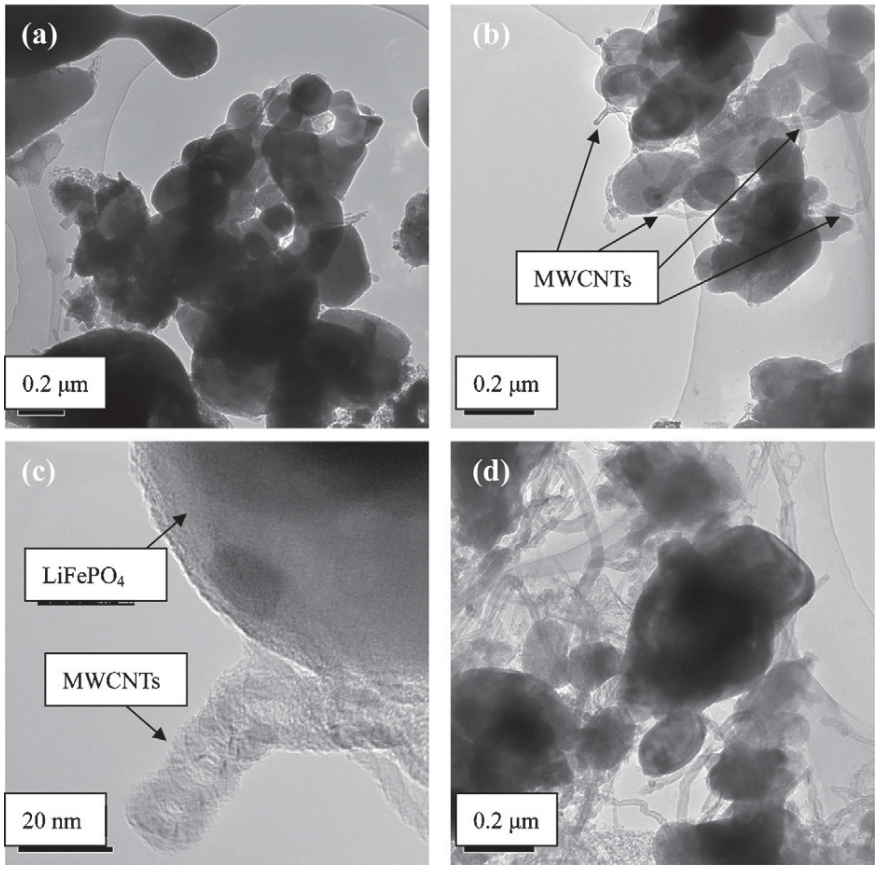

Fig. 3. TEM images of $LiFePO_4$ (a), $LiFePO_4$/7 wt.% MWCNTs (b and c) and $LiFePO_4$/7 wt.% MWCNTs (d).

for $LiFePO_4$/7 wt.% MWCNTs, while the discharge voltage plateau is 3.31–3.33 V for $LiFePO_4$ and 3.37–3.40 V for sample $LiFePO_4$ 7 wt.% MWCNTs. The lower electrochemical polarization of the MWCNTs coating composites suggests that the increased conductivity is induced. The dispersed MWCNTs networks promote the electrochemical reaction by enhancing the composite electronic conduction.

CV profiles of $LiFePO_4$ and $LiFePO_4$/7 wt.% MWCNTs are shown in Fig. 7. The lithium intercalation ($LiFePO_4$ reduction) and extraction ($LiFePO_4$ oxidation) peaks of $LiFePO_4$ are located at 3.23 and 3.58 V vs. Li^+/Li respectively while those of $LiFePO_4$ with 7 wt.% MWCNTs are at 3.32 and 3.54 V vs. Li^+/Li. Noticeably, the peak distance of $LiFePO_4$ with 7 wt.% MWCNTs is less than that of pure $LiFePO_4$, which suggests the $LiFePO_4$ with 7 wt.% MWCNTs composite has better electrochemical reversibility than $LiFePO_4$. Broadened peaks of $LiFePO_4$ show poor kinetics (the sluggish lithium intercalation and extraction), while sharp peaks of $LiFePO_4$ with 7 wt.% MWCNTs composite show excellent kinetics (the facile lithium intercalation and extraction). That concludes WMCNTs coating can improve the electrochemical reversibility and kinetics of $LiFePO_4$ cathodes materials.

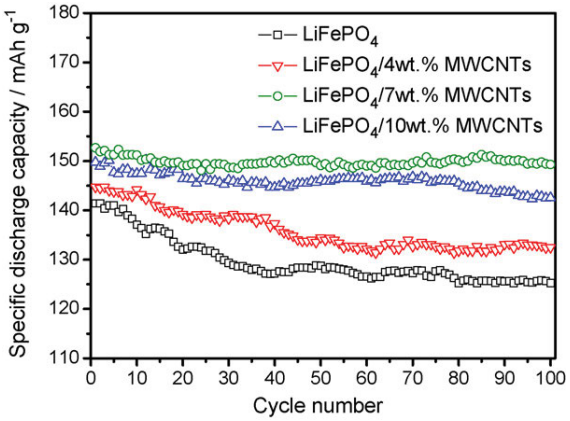

Fig. 4. Discharge capacities of $LiFePO_4$ and $LiFePO_4$-MWCNTs. Rate: 0.18 C (1 C = 170 mA g^{-1}); cut-offs: 2.5 and 4.3 V vs. Li^+/Li.

EIS tests were carried out to evaluate the electrochemical kinetics properties of the as-prepared materials. Fig. 8 shows the Nyquist plots of the experimental data and fitting results of pure $LiFePO_4$ and $LiFePO_4$ with 7 wt.% MWCNTs. Each of the spectra consists of a depressed semicircle attributed to the charge transfer process and a linear Warburg part attributed to the diffusion of the lithium ions in the bulk of the electrode. The semicircle attributed to SEI layer was not observed. The fitting results were obtained by ZView from Sai software set [41] using an electrochemical model (equivalent circuit) shown in Fig. 8. Where R_0 represents the sum of the ohmic resistance of the research system, including the ohmic resistance of the electrolyte, the electrode, the interface, etc., CPE (constant

Table 2
EIS fitting results of $LiFePO_4$ and $LiFePO_4$/7 wt.% MWCNTs.

Parameter	$LiFePO_4$	$LiFePO_4$/7 wt.% MWCNTs
R_0/Ω	5.686	4.246
R_{ct}/Ω	264.2	101.2
CPE-T/μF	9.351	19.78
Ws-R/Ω	1481	61.15

Samsung Ex. 1042, Page 4 of 6
Samsung Electronics Co., Ltd., et al. v. Molecular Rebar Design, LLC
IPR2025-00356

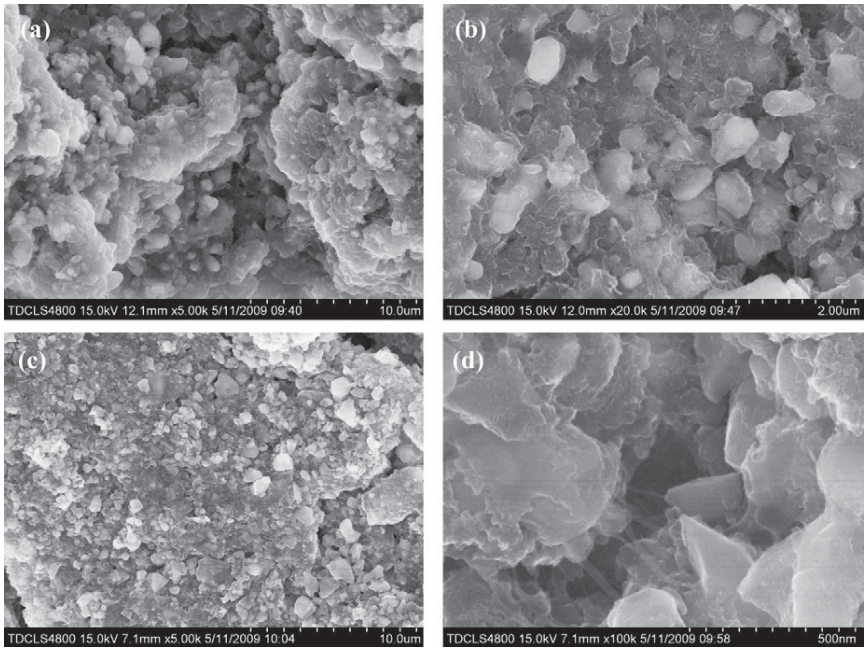

Fig. 5. SEM images of $LiFePO_4$ (a and b) and $LiFePO_4$/7 wt.% MWCNTs composites (c and d) after 100 cycles charge–discharge.

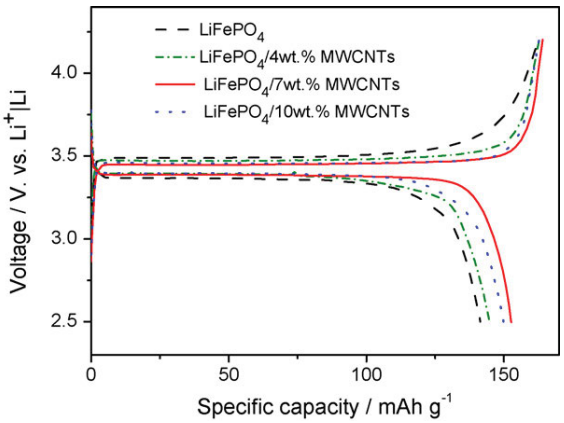

Fig. 6. The initial voltage profiles of $LiFePO_4$ and $LiFePO_4$-MWCNTs. (0.18 C).

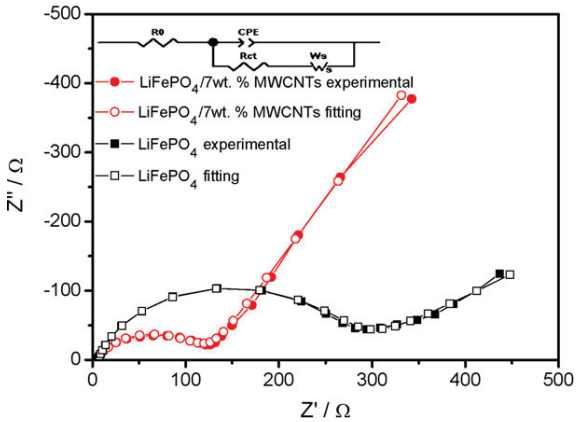

Fig. 8. EIS Nyquist plots of experimental data and fitting results of $LiFePO_4$ and $LiFePO_4$/7 wt.% MWCNTs electrodes and equivalent circuit for EIS data fitting (sub figure).

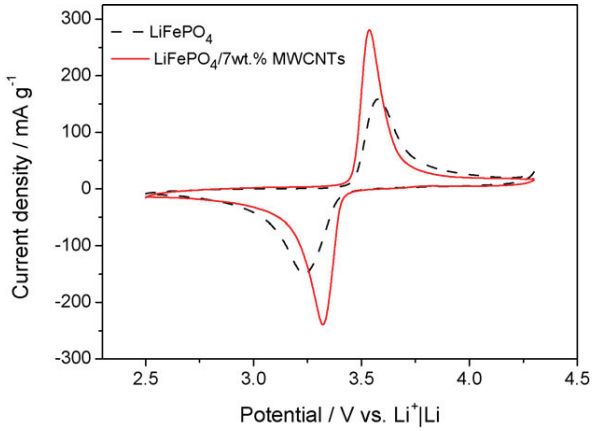

Fig. 7. CV curves of $LiFePO_4$ and $LiFePO_4$/7 wt.% MWCNTs composite electrodes at a scan rate of 0.1 mV s^{-1} (voltage range: 2.5–4.3 V).

phase element) represents the double layer capacitance and the SEI film capacitance instead of a capacitor to compensate for non-homogeneity in the system, R_{ct} is a charge transfer resistor and W_s is the finite length Warburg with a short circuit terminus. Some of the parameters obtained by fitting are listed in Table 2. Compared with the EIS fitting data of pure $LiFePO_4$, $LiFePO_4$ with 7 wt.% MWCNTs exhibited smaller R_{ct} value indicating faster electrochemical kinetics, larger double layer capacitance CPE-T (greater lithium ion diffusion capability) and smaller diffusion resistance Ws-R for lithium ions indicating larger electrochemical active specific surface area [42].

4. Conclusion

$LiFePO_4$-MWCNTs as cathode materials for lithium ion batteries were successfully synthesized by mixing $LiFePO_4$ and MWCNTs in ethanol and followed by heat-treatment. The MWCNTs did not influence the phase structure of $LiFePO_4$ but coated on the $LiFePO_4$

Samsung Ex. 1042, Page 5 of 6
Samsung Electronics Co., Ltd., et al. v. Molecular Rebar Design, LLC
IPR2025-00356

particles. The MWCNTs connecting the particles with strong webs to make the structure of the cathode material stable during the charge–discharge cycling. MWCNTs adding improved the electronic conductivity, the discharge capacity, cycle stability and electrochemical kinetics of $LiFePO_4$. In all these prepared $LiFePO_4$ with x wt.% MWCNTs (x = 4, 7, 10) composites, 7 wt.% MWCNTs adding composite cathode shows the best electrochemical performance, which gets an initial discharge capacity of 152.7 mAh g^{-1} at 0.18 C discharge rates with capacity retention ratio of 97.77% after 100 cycles, showing it is a promising cathode material for lithium ion batteries.

Acknowledgement

This work was financially supported by the Talent Fund Projects for Introduced Scholar in Tianjin Normal University.(No. 5RL089). The author thanks Dr. Ming Zhao at Tianjin B&M Science and Technology Joint-Stock Company for helpful discussions.

References

[1] M.K. Datta, P.N. Kumta, J. Power Sources 165 (2007) 368.
[2] X.Y. Han, C. Chang, L.J. Yuan, T. Sun, J.T. Sun, Adv. Mater. 19 (2007) 1616.
[3] J.T. Son, E.J. Cairns, J. Power Sources 166 (2007) 343.
[4] A. Deb, U. Bergmann, S.P. Cramer, E.J. Cairns, J. Electrochem. Soc. 154 (2007) A534.
[5] H.Y. Park, S.C. Nam, Y.C. Lim, K.G. Choi, K.C. Lee, G.B. Park, J.B. Kim, H.P. Kim, S.B. Cho, Eletrochim. Acta 52 (2007) 2062.
[6] H.W. Liu, C.X. Cheng, Z.Q. Hu, K.L. Zhang, Mater. Chem. Phys. 101 (2007) 276.
[7] K.S. Lee, S.T. Myung, H.J. Bang, S.J. Chung, Y.K. Sun, Electrochim. Acta 52 (2007) 5201.
[8] B.L. He, W.J. Zhou, S.J. Bao, Y.Y. Liang, H.L. Li, Electrochim. Acta 52 (2007) 3286.
[9] D.G. Tang, Y.X. Ci, Q. Lu, J. Solid State Electrochem. 11 (2007) 350.
[10] X.F. Li, Y.L. Xu, Electrochem. Commun. 9 (2007) 2023.
[11] T. Kakuda, K. Uematsu, K. Toda, M. Sato, J. Power Sources 167 (2007) 499.
[12] A. Subramania, N. Angayarkanni, T. Vasudevan, Mater. Chem. Phys. 102 (2007) 19.
[13] R. Singhal, S.R. Das, M.S. Tomar, O. Ovideo, S. Nieto, R.E. Melgarejo, R.S. Katiyar, J. Power Sources 164 (2007) 857.
[14] K.M. Shaju, P.G. Bruce, Adv. Mater. 18 (2006) 2330.
[15] S. Zhang, Electrochim. Acta 52 (2007) 7337.
[16] Y.H. Ding, P. Zhang, Y. Jiang, D. Gao, Solid State Ionics 178 (2007) 967.
[17] Y.S. He, Z.F. Ma, X.Z. Liao, Y. Jiang, J. Power Sources 163 (2007) 1053.
[18] W. Lu, J. Liu, Y.K. Sun, K. Amine, J. Power Sources 167 (2007) 212.
[19] L.F. Jiao, M. Zhang, H.T. Yuan, M. Zhao, J. Guo, W. Wang, X.D. Zhou, Y.M. Wang, J. Power Sources 167 (2007) 178.
[20] L.Q. Wang, L.F. Jiao, H.T. Yuan, J. Guo, M. Zhao, H.X. Li, Y.M. Wang, J. Power Sources 162 (2006) 1367.
[21] M. Zhao, L.F. Jiao, H.T. Yuan, Y. Feng, M. Zhang, Solid State Ionics 178 (2007) 387.
[22] M. Schindler, F.C. Hawthorne, M.A. Alexander, R.A. Kutluoglu, P. Mandaliev, N.M. Halden, R.H. Mitchell, J. Solid State Chem. 179 (2006) 2616.
[23] Y.S. Hu, Y.G. Guo, R. Dominko, M. Gaberscek, J. Jamnik, J. Maier, Adv. Mater. 19 (2007) 1963.
[24] R. Dominko, M. Bele, J.M. Goupil, M. Gaberscek, D. Hanzel, I. Arcon, J. Jamnik, Chem. Mater. 19 (2007) 2960.
[25] L.M. Moshurchak, C. Buhrmester, R.L. Wang, J.R. Dahn, Electrochim. Acta 52 (2007) 3779.
[26] C.H. Mi, X.G. Zhang, H.L. Li, J. Electroanal. Chem. 602 (2007) 245.
[27] D. Choi, P.N. Kumta, J. Power Sources 163 (2007) 1064.
[28] M. Zhang, L.F. Jiao, H.T. Yuan, Y.M. Wang, J. Guo, M. Zhao, W. Wang, X.D. Zhou, Solid State Ionics 177 (2006) 3309.
[29] R.G. Hu, X.G. Gao, Z.D. Peng, K. Du, X.Y. Tan, Y.J. Liu, Trans. Noferrous Met. Soc. China 17 (2007) 296.
[30] G.X. Wang, L. Yang, Y. Chen, J.Z. Wang, S. Bewlay, H.K. Liu, Electrochim. Acta 50 (2005) 4649.
[31] Y.H. Huang, K.S. Park, J.B. Goodenough, J. Electrochem. Soc. 153 (2006) A2282.
[32] X.L. Li, F.Y. Kang, X.D. Bai, W.C. Shen, Electrochem. Commun. 9 (2007) 663.
[33] D.J. Yang, S.G. Wang, Q. Zhang, Phys. Lett. A 329 (2004) 207.
[34] A. Thess, R. Lee, P. Nikolaev, Science 273 (1996) 483.
[35] Y.J. Liu, X.H. Li, H.J. Guo, Z.X. Wang, W.J. Peng, Y. Yang, R.F. Liang, J. Powers Sources 184 (2008) 522.
[36] K. Sheem, Y.H. Lee, H.S. Lim, J. Power Sources 158 (2006) 1425.
[37] J.J. Chen, M.S. Whittingham, Electrochem. Commun. 8 (2006) 855.
[38] B. Jin, E.M. Jin, K.H. Park, H.B. Gu, Electrochem. Commun. 10 (2008) 1537.
[39] L. Wang, Y.D. Huang, R.R. Jiang, J. Electrochem. Soc. 154 (2007) A1015.
[40] A.S. Andersson, B. Kalska, L. Haggstrom, J.O. Thomas, Solid State Ionics 130 (2000) 41.
[41] Y. Feng, L.F. Jiao, H.T. Yuan, M. Zhao, Int. J. Hydrogen Energy 32 (2007) 2836.
[42] M. Zhao, L.F. Jiao, H.T. Huan, J.L. Sun, Y. Feng, Chin. J. Chem. 26 (2008) 290.

Samsung Ex. 1042, Page 6 of 6
Samsung Electronics Co., Ltd., et al. v. Molecular Rebar Design, LLC
IPR2025-00356